J Magn Reson Imaging **24**: 1133-1139, 2006

〔29〕 Lorenz C, Benner T, Lopez CJ et al: Effect of using local arterial input functions on cerebral blood flow estimation. J Magn Reson Imaging **24**: 57-65, 2006

〔30〕 Murase K, Kikuchi K, Miki H et al: Determination of arterial input function using fuzzy clustering for quantification of cerebral blood flow with dynamic susceptibility contrast-enhanced MR imaging. J Magn Reson Imaging **13**: 797-806, 2001

〔31〕 Mouridsen K, Christensen S, Gyldensted L et al: Automatic selection of arterial input function using cluster analysis. Magn Reson Med **55**: 524-531, 2006

〔32〕 van Osch MJ, Vonken EJ, Viergever MA et al: Measuring the arterial input function with gradient echo sequences. Magn Reson Med **49**: 1067-1076, 2003

〔33〕 Akbudak E, Conturo TE: Arterial input functions from MR phase imaging. Magn Reson Med **36**: 809-815, 1996

〔34〕 Akbudak E, Norberg RE, Conturo TE: Contrast-agent phase effects: an experimental system for analysis of susceptibility, concentration, and bolus input function kinetics. Magn Reson Med **38**: 990-1002, 1997

〔35〕 Conturo TE, Akbudak E, Kotys MS et al: Arterial input functions for dynamic susceptibility contrast MRI: requirements and signal options. J Magn Reson Imaging **22**: 697-703, 2005

〔36〕 Vonken EJ, van Osch MJ, Bakker CJ et al: Measurement of cerebral perfusion with dual-echo multi-slice quantitative dynamic susceptibility contrast MRI. J Magn Reson Imaging **10**: 109-117, 1999

〔37〕 Ostergaard L, Sorensen AG, Kwong KK et al: High resolution measurement of cerebral blood flow using intravascular tracer bolus passages. Part II: Experimental comparison and preliminary results. Magn Reson Med **36**: 726-736, 1996

〔38〕 Ellinger R, Kremser C, Schocke MF et al: The impact of peak saturation of the arterial input function on quantitative evaluation of dynamic susceptibility contrast-enhanced MR studies. J Comput Assist Tomogr **24**: 942-948, 2000

〔39〕 Lin W, Celik A, Derdeyn C et al: Quantitative measurements of cerebral blood flow in patients with unilateral carotid artery occlusion: a PET and MR study. J Magn Reson Imaging **14**: 659-667, 2001

〔40〕 van Osch MJ, van der Grond J, Bakker CJ: Partial volume effects on arterial input functions: shape and amplitude distortions and their correction. J Magn Reson Imaging **22**: 704-709, 2005

〔41〕 van Osch MJ, Vonken EJ, Bakker CJ et al: Correcting partial volume artifacts of the arterial input function in quantitative cerebral perfusion MRI. Magn Reson Med **45**: 477-485, 2001

〔42〕 圓見純一郎，佐藤博司，山本明秀，他：DSC-MRIによる脳血流量測定における動脈入力関数推定方法に関する検討．第35回日本磁気共鳴医学会大会講演抄録集，2007, pp425

〔43〕 Ostergaard L, Weisskoff RM, Chesler DA et al: High resolution measurement of cerebral blood flow using intravascular tracer bolus passages. Part I: Mathematical approach and statistical analysis. Magn Reson Med **36**: 715-725, 1996

〔44〕 Stewart GN: Researches on the circulation time in organs and on the influences which affect it. Parts I-III. J Physiol **15**: 1, 1894

〔45〕 Meier P, Zierler KL: On the theory of the indicator-dilution method for measurement of blood flow and volume. J Appl Physiol **6**: 731-744, 1954

〔46〕 Calamante F, Gadian DG, Connelly A: Delay and dispersion effects in dynamic susceptibility contrast MRI: simulations using singular value decomposition. Magn Reson Med **44**: 466-473, 2000

〔47〕 Wu O, Ostergaard L, Koroshetz WJ et al: Effects of tracer arrival time on flow estimates in MR perfusion-weighted imaging. Magn Reson Med **50**: 856-864, 2003

〔48〕 Wu O, Ostergaard L, Weisskoff RM et al: Tracer arrival timing-insensitive technique for estimating flow in MR perfusion-weighted imaging using singular value decomposition with a block-circulant deconvolution matrix. Magn Reson Med **50**: 164-174, 2003

〔49〕 Smith MR, Lu H, Trochet S et al: Removing the effect of SVD algorithmic artifacts present in quantitative MR perfusion studies. Magn Reson Med **51**: 631-634, 2004

〔50〕 Calamante F, Morup M, Hansen LK: Defining a local arterial input function for perfusion MRI using independent component analysis. Magn Reson Med **52**: 789-797, 2004

〔51〕 Smith M, Salluzzi M, Frayne R: Adaptive SVD thresholding is shown to be more appropriate for partial brain scans (TR = 1 s) rather than full brain scans (TR = 2 s). the ISMRM 14th Annual Meeting, 2006, pp 1541

圓見純一郎（えんみ　じゅんいちろう）
2000年北海道大学大学院理学研究科化学第二専攻博士後期課程修了．同年千歳科学技術大学光科学部特別研究員．2001年㈱日本アレフ入社．同年（財）医療機器センター流動研究員（国立循環器病センター研究所放射線医学部へ派遣）．2004年国立循環器病センター流動研究員．2007年国立循環器病センター特任研究員．日本磁気共鳴医学会会員．

*　　*　　*

Stroke
JOURNAL OF THE AMERICAN HEART ASSOCIATION

American Stroke Association
A Division of American Heart Association

Delayed Postischemic Treatment With Fluvastatin Improved Cognitive Impairment After Stroke in Rats

Munehisa Shimamura, Naoyuki Sato, Masataka Sata, Hitomi Kurinami, Daisuke Takeuchi, Kouji Wakayama, Takuya Hayashi, Hidehiro Iida and Ryuichi Morishita

Stroke published online Nov 1, 2007;
DOI: 10.1161/STROKEAHA.107.485045
Stroke is published by the American Heart Association. 7272 Greenville Avenue, Dallas, TX 72514
 Print ISSN: 0039-2499. Online ISSN: 1524-4628

Delayed Postischemic Treatment With Fluvastatin Improved Cognitive Impairment After Stroke in Rats

Munehisa Shimamura, MD, PhD; Naoyuki Sato, MD, PhD; Masataka Sata, MD, PhD; Hitomi Kurinami, MD; Daisuke Takeuchi, MD; Kouji Wakayama, MD; Takuya Hayashi, MD, PhD; Hidehiro Iida, MD, PhD; Ryuichi Morishita, MD, PhD

Background and Purposes—Recent clinical evidences indicate that statins may have beneficial effects on the functional recovery after ischemic stroke. However, the effect of delayed postischemic treatment with statins is still unclear. In the present study, we evaluated the effects of fluvastatin in the chronic stage of cerebral infarction in a rat model.

Methods—Rats exposed to permanent middle cerebral artery occlusion were treated for 3 months with fluvastatin beginning from 7 days after stroke. MRI, behavioral analysis, and immunohistochemistry were performed.

Results—Two months of treatment with fluvastatin showed the significant recovery in spatial learning without the decrease in serum total cholesterol level and worsening of infarction. Microangiography showed a significant increase in capillary density in the peri-infarct region in fluvastatin-treated rats after 3 months of treatment. Consistently, BrdU/CD31-positive cells were significantly increased in fluvastatin-treated rats after 7 days of treatment. MAP1B-positive neurites were also increased in the peri-infarct region in fluvastatin-treated rats. In addition, rats treated with fluvastatin showed the reduction of superoxide anion after 7 days of treatment and the reduction of Aβ deposits in the thalamic nuclei after 3 months of treatment.

Conclusions—Thus, delayed postischemic administration of fluvastatin had beneficial effects on the recovery of cognitive function without affecting the infarction size after ischemic stroke. Pleiotropic effects of fluvastatin, such as angiogenesis, neuritogenesis, and inhibition of superoxide production and Aβ deposition, might be associated with a favorable outcome. (***Stroke*. 2007;38:000-000.)**

Key Words: angiogenesis ■ cerebral infarct ■ microcirculation ■ statins

Despite conflicting data correlating cholesterol level with stroke, 2 early trials of HMG-CoA reductase inhibitors (statins) in patients after myocardial infarction patients showed a reduction in stroke risk as a secondary end point.[1] A meta-analysis of 9 statin intervention trials, which enrolled patients with coronary artery disease or those at high risk for coronary disease, demonstrated a 21% relative risk reduction for stroke after 5 years of treatment.[2] Another clinical evidence suggests that the commencement of statins within 4 weeks of a stroke results in a favorable 90-day outcome.[3] To clarify the effects of postischemic statin treatment, previous studies in which atorvastatin was started 1 day after stroke in rodents showed improvement of sensory motor deficit through induction of angiogenesis, neurogenesis, and synaptogenesis.[4,5] These pleiotropic effects of statins were shown to be the result of induction of vascular endothelial growth factor or brain-derived neurotrophic factor.[4] Additionally, the microvascular dysfunction in the posttreatment of stroke with recombinant human tissue-type plasminogen activator could be reduced by statins in rodent model.[6] However, the effect of delayed treatment with statins after ischemic stroke is still unknown. From this viewpoint, we investigated whether chronic statin treatment beginning 7 days after ischemic stroke had influences on neurological deficits and pathophysiology after the permanent middle cerebral artery occlusion (MCAo) model in rats.

Materials and Methods

Surgical Procedure

Male Wistar rats (270 to 300 grams; Charles River; Kanagawa, Japan) were used in this study. The right MCA was occluded by placement of poly-L-lysine–coated 4-0 nylon, as described previously.[7]

Protocol for Treatment and Behavioral Tests

Ten rats were only anesthetized (sham operation) and 32 rats were subjected to MCAo (day 1). Based on neuromuscular function on day 7, the rats were divided equally into saline-treated (n=16) or fluvastatin-treated (n=16) groups. Fluvastatin (5 mg/kg per day;

Received February 14, 2007; final revision received April 27, 2007; accepted May 30, 2007.

From Department of Advanced Clinical Science and Therapeutics (M.S., M.Sata, K.W.), Graduate School of Medicine, the University of Tokyo, Japan; Department of Clinical Gene Therapy (N.S., H.K., D.T., R.M.), Graduate School of Medicine, Osaka University, Japan; Department of Investigative Radiology (T.H., H.I.), National Cardiovascular Center, Research Institute, Japan.

Correspondence to Ryuichi Morishita, MD, PhD, Professor, Division of Clinical Gene Therapy, Graduate School of Medicine, Osaka University, 2-2 Yamada-oka, Suita 565-0871, Japan. E-mail morishit@cgt.med.osaka-u.ac.jp

Stroke **is available at http://stroke.ahajournals.org** **DOI: 10.1161/STROKEAHA.107.485045**

provided by Novartis Pharma) or saline was given by gavage from day 7 to 100. We chose the dose (5 mg/kg per day), because a previous report showed that this dose could effectively induce angiogenesis in ischemic limb.[8] On day 55, neuromuscular function and locomotor activity were evaluated in the surviving rats. Then, cognitive function was examined by Morris water maze from day 56 to 63, because the effects of neuronal regeneration could be detected not in the early stage but in the chronic stage of ischemic brain such as 49 to 53 days after the insult.[9] On day 96, MRI was performed. On day 100, microangiography was performed.

MRI

High-resolution T1-weighted fast spin echo sequence images (repetition time [TR]=1500 ms; echo time [TE]=10.3 ms; field of view [FOV]=4× 3 cm; matrix=256×192; slice thickness=1.5 mm; slice gap=0.5 mm; number of slices=16; number of excitation=10; total time=9.39 min) were obtained using a 3-T MRI scanner (Signa LX VAH/I; GE).

Sensory Motor Deficit and Locomotor Activity

Although there are various batteries for testing sensory motor deficit, we used a simple protocol.[10] For forelimb flexion, rats were held by the tail on a flat surface. Paralysis of the forelimbs was evaluated by the degree of left forelimb flexion. For torso twisting, rats were held by the tail on a flat surface. The degree of body rotation was checked. For lateral push, rats were pushed either left or right. Rats with right MCA occlusion showed weak or no resistance against a left push. For hind limb placement, one hind limb was removed from the surface. Rats with right MCA occlusion showed delayed or no replacement of the hind limb when it was removed from the surface.

Spontaneous activity was measured via the open field (0.69 m^2). We set the sensor, which also put beams on the field, at 30 cm above the field. The number of count, which is when the animal crosses the beam, was measured for 30 minutes.

Morris Water Maze Task

A cylindrical tank 1.5 m in diameter was filled with water (25°C), and a transparent platform 15 cm in diameter was placed at a fixed position in the center of 1 of the 4 quadrants (O'Hara & Co, Ltd). In the hidden platform trials, we performed the tests 4 times per day for 4 days. When the rat could not reach the platform, the latency was set at 60 sec. In the visible platform trials, the tests were performed 4 times per day for 4 days. The acquired data were averaged per day.

Evaluation of Capillary Density

Using a recently developed microangiographic technique,[11] capillary density and blood–brain barrier leakage were evaluated in the cerebral cortex after MCA occlusion. The area or length of vessels was analyzed with an angiogenesis image analyzer (version 1.0; Kurabo).

Immunohistochemical Study: Bromodeoxyuridine Labeling

To identify newly formed DNA, saline-treated (n=5) and fluvastatin-treated (n=5) rats received injections of bromodeoxyuridine (BrdU, 50 mg/kg; Sigma-Aldrich, Saint Louis, Mo) intraperitoneally starting on day 7 twice per day until day 13. Rats were euthanized on day 14. After the sections (8-μm thickness) was fixed in 10% formaldehyde/MeOH neutral buffer solution and blocked, they were incubated with mouse monoclonal anti-rat CD31 antibody (1:100; BD Biosciences; San Jose, Calif), goat polyclonal anti-doublecortin (anti-DCX; Santa Cruz) antibody (1:100; Santa Cruz, Calif), mouse monoclonal anti-NeuN antibody (1:1000; Chemicon, Temecula, Calif), or mouse monoclonal anti-MAP1B antibody (1:100; Sigma-Aldrich), followed by anti-mouse goat fluorescent antibody (1:1000 for NeuN and MAP1B, 1:400 for CD31, Alexa Flour 546, Molecular Probes; Eugene, Ore) or anti-goat donkey fluorescent antibody (1:1000 for DCX Alexa Fluor 546). For double immunostaining, these sections were fixed again and incubated in 2 N HCl at 37°C for 30 minutes. After blocking, they were incubated with rat monoclonal anti-BrdU antibody (1:200; Abcam, Cambridge, UK) followed by anti-rat goat fluorescent antibody (1:1000, Alexa Fluor 488). For immunohistochemical staining for Aβ, sections were pretreated for 30 minutes with hot (85°C) citrate buffer as described before.[12] Confocal images were acquired using an FV-300 (Olympus).

Table. Infarction Volume Calculated by MRI, Blood Pressure, and Serum Total Cholesterol

	Sham	MCAo+S	MCAo+F	*P*
Infarction volume in total rats (mm^3)	...	283.8±23.9	278.4±26.4	0.851
Type of infarction in Figure 1a (N of rats)				0.828
A	...	12	11	...
B	...	3	3	...
C	...	1	2	...
Infarction volume (mm^3) in type A rats	...	322.8±15.0	327.0±18.8	0.758
Systolic blood pressure (mm Hg) in type A rats				
Day 7	116.1±5.4	123.7±6.0	115.5±7.3	0.654
Day 56	146.5±4.7	148.3±2.7	136.1±5.2	0.132
Serum total cholesterol (mg/dl) in type A rats on day 56	85.9±5.6	75.3±3.5	73.5±2.7	0.949

Type A, low-intensity area seen in the dorsolateral and lateral portions of the neocortex and the entire caudate putamen; type B, low-intensity area seen in the dorsolateral and lateral portions of the neocortex and in part of the caudate putamen; type C, low-intensity area seen in part of the lateral neocortex and caudate putamen. MCAo+S, saline-treated rats after MCAo; MCAo+F, fluvastatin-treated rats after MCAo.

P, saline vs fluvastatin.

Quantitative Histological Analysis

To quantify the immunoreactivity for MAP1B and Aβ, the acquired image was analyzed by Image J (version 1.32; NIH).

Detection of Superoxide Anion in Brain Sections

Superoxide anion was detected on day 14 as described previously.[13] Because intact cortex showed red fluorescence, we calculated the ratio of fluorescence as follows: ratio of fluorescence=[fluorescence intensity in ischemic core or peri-infarct region]/[fluorescence intensity in intact region].

Statistical Analysis

All values are expressed as mean±SEM. To analyze the differences in the type of cerebral infarction, χ^2 test was performed. The latency, path length, and mean speed in Morris water maze and sensory motor deficits were analyzed by a 2-factor repeated-measure ANOVA. Post hoc analyses were performed, and the Scheffe test was applied to control the inflation in type I error. The value of the serum total cholesterol, the blood pressure, and the spontaneous activity was analyzed by Scheffe rules. The differences in the immunohistochemistry and the volume of infarction were assessed by Mann–Whitney *U* analyses. In all cases, $P<0.05$ was considered significant.

Results

Effects of Fluvastatin on Cognitive Impairment

To confirm the severity of cerebral infarction, all rats were examined by T1-weighted MRI after 89 days of treatment. Although the total volume of infarction calculated in T1-weighted images was not different between rats treated with

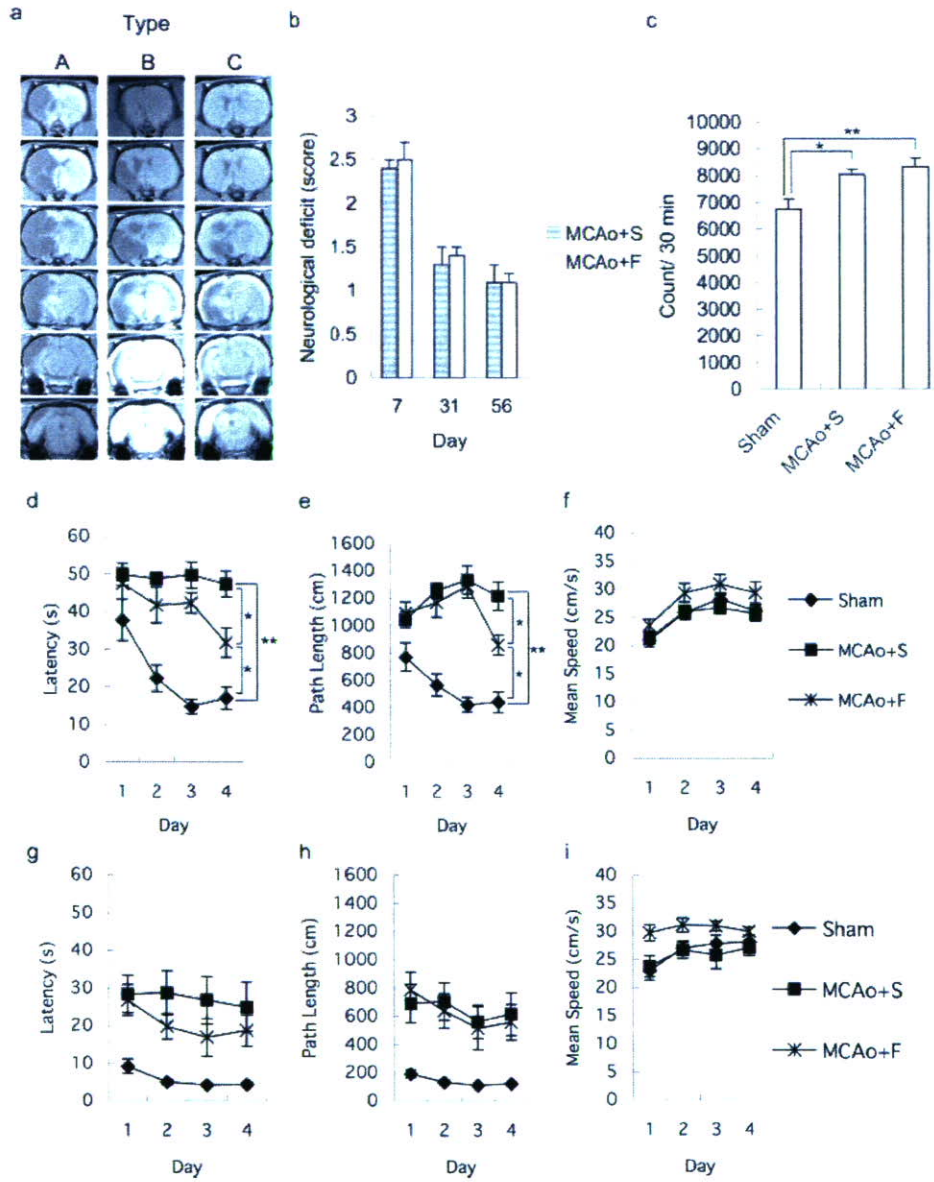

Figure 1. Typical T1-weighted image of coronal section of rat brain (a). The images were divided into 3 groups. Type A, low-intensity area seen in the dorsolateral and lateral portions of neocortex and the entire caudoputamen; type B, low-intensity area seen in the dorsolateral and lateral portions of neocortex and in part of the caudatoputamen; and type C, high-intensity area seen in part of the lateral neocortex and caudatoputamen. Sensory motor deficit (b). Spontaneous locomotor activity (c). Hidden platform test in Morris water maze. Each figure showed latency (d), path length (e), and mean speed (f). Days 1 to 4 indicate the trial day in the hidden platform test (56 to 59 days after middle cerebral artery occlusion). Visible platform test in Morris water maze. Each figure showed latency (g), path length (h), and mean speed (i). Days 1 to 4 indicate the day in the visible platform test (60 to 63 days after middle cerebral artery occlusion). MCAo+S indicates rats treated with saline after middle cerebral artery occlusion; MCAo+F, rats treated with fluvastatin after middle cerebral artery occlusion.

saline and fluvastatin (Table), the pattern of cerebral infarction was divided into 3 groups: type A, low-intensity area seen in the dorsolateral and lateral portions of the neocortex and the entire caudate putamen; type B, low-intensity area seen in the dorsolateral and lateral portions of the neocortex and in part of the caudate putamen; type C, low-intensity area seen in part of the lateral neocortex and caudate putamen (Figure 1a). In type C, most of the lateral neocortex was intact. To exclude the influence of the pattern of cerebral infarction on cognitive function, we focused on type A rats in the present study. The volume of cerebral infarction in type A rats was not different between the groups (Table). Blood pressure and serum total cholesterol also showed no difference among the groups (Table).

Sensory motor deficit had spontaneously recovered to some extent by 8 weeks in both groups, and there was no difference (Figure 1b). Locomotor activity in rats subjected to MCAo was increased as compared with that in sham-operated rats, as described before,[14] but there was no significant difference between fluvastatin-treated and saline-treated rats (Figure 1c). In Morris water maze (Figure 1d-i), which examines spatial learning, there were significant differences

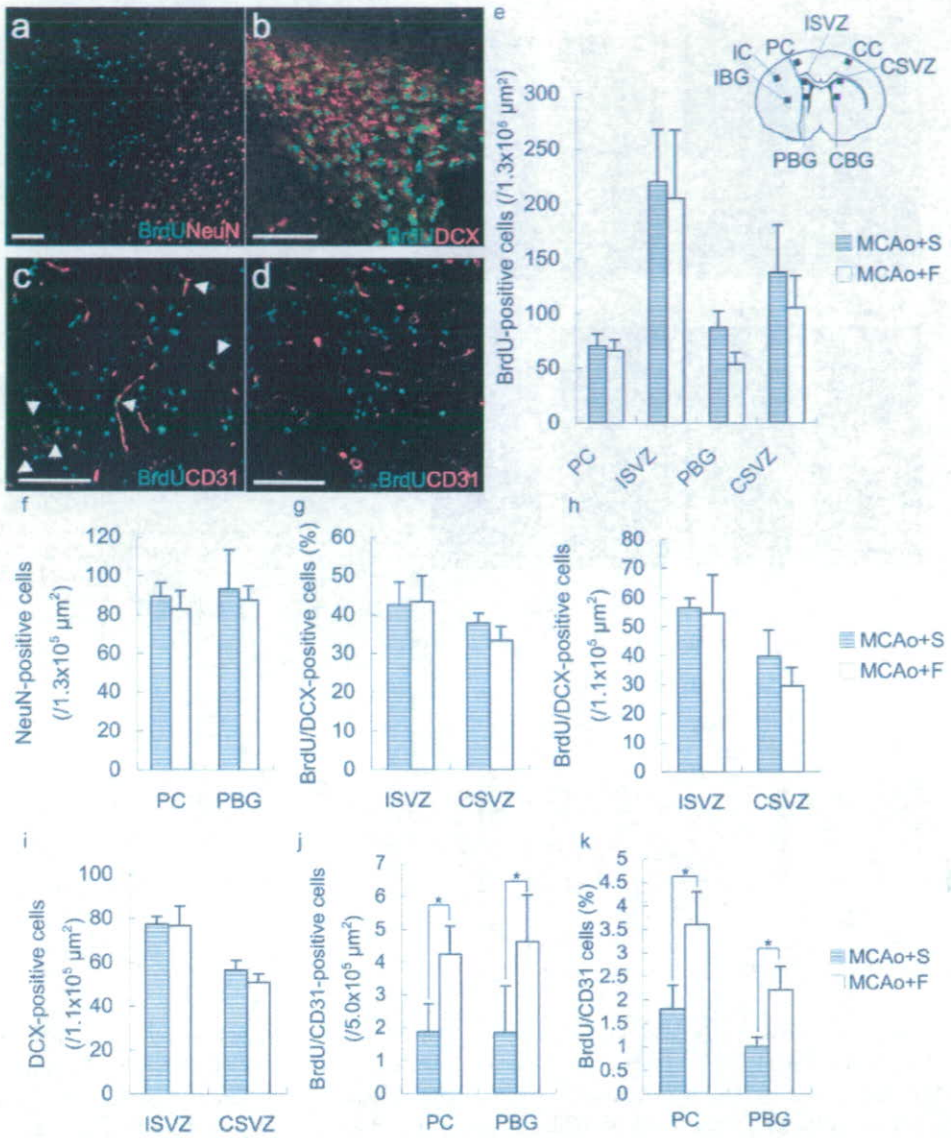

Figure 2. Representative images of immunohistochemical staining on day 14. Rats treated with fluvastatin (a through c), rats treated with saline (d). Although BrdU-positive cells were observed in the peri-infarct cortex (a), peri-infarct basal ganglia, and subventricular zone, these cells did not express NeuN (a), but expressed DCX in the subventricular zone (b). Fluvastatin-treated rats showed some BrdU/CD31-positive cells (arrows, c), although most BrdU-positive cells were negative for CD31 in saline-treated rats (d). The number of BrdU-positive cells (e), NeuN-positive cells (f), BrdU/DCX-positive cells (h), DCX-positive cells (i), and BrdU/CD31-positive cells (j); the percentage of BrdU/DCX-positive cells (g) or BrdU/CD31 cells (k) in total BrdU-positive cells. PC indicates peri-infarct cortex; PBG, peri-infarct basal ganglia; IC, infarcted cortex; IBG, ischemic basal ganglia; ISVZ, subventricular zone on infarcted side; CC, contralateral cortex, CSVZ, subventricular zone on contralateral side; CBG, contralateral basal ganglia (n=5 in each group, $^*P<0.05$, bar=100 μm).

in the latency and path length in hidden platform test among the groups (supplemental Table I, available online at http://stroke.ahajournals.org). A significant difference was observed on day 4 between fluvastatin-treated and saline-treated rats (supplemental Table I). Also, there was a significant difference between sham and saline-treated rats (supplemental Table I). There was no significant difference both in swimming speed and visible platform test, which excluded the possible influence of visual loss, sensory motor deficit, and motivation on the results.[15] These data suggest that impaired spatial learning was improved by fluvastatin.

Histological Changes by Fluvastatin

Next, we studied whether fluvastatin had some influences on the histology. Initially, we focused on neurogenesis and angiogenesis. To examine neurogenesis, we measured BrdU-incorporated cells after injecting BrdU from day 7 to day 13. Although BrdU-positive cells were observed in the subventricular zone and peri-infarct region (Figure 2a to 2d), the total number did not differ between the groups (Figure 2e). Similarly, the density of NeuN-positive cells, as a marker of adult neurons, also did not differ between the groups (Figure 2f), whereas there were no BrdU/NeuN-positive cells in the

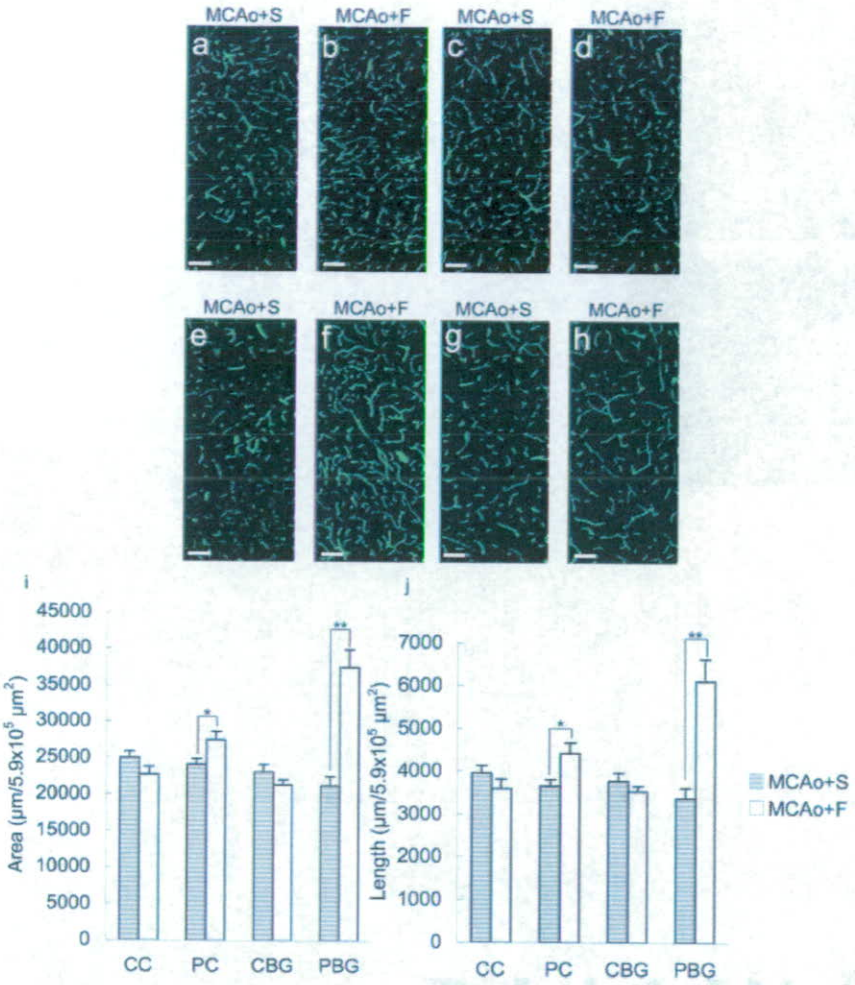

Figure 3. Microangiographic images using albumin-fluorescence isothiocyanate on day 100: (a and b) peri-infarct cortex; (c and d) contralateral cortex; (e and f) peri-infarct basal ganglia; (g and h) contralateral basal ganglia (bar=100 μm). Quantitative analysis (i and j) of microangiography. Rats treated with fluvastatin showed increased microvessels in the peri-infarct region (n=4 in each group, $^{*}P<0.05$, $^{**}P<0.01$).

peri-infarct cortex and subventricular zone (Figure 2a). Although some BrdU-positive cells expressing DCX, a marker for migrating neuroblasts, could be detected in subventricular zone (Figure 2b), the percentage in total BrdU-positive cells (Figure 2g) and the number (Figure 2h) did not differ between the groups. Also, the number of DCX-positive cells was same in the both groups (Figure 2i). There were no BrdU-positive cells expressing DCX in the cerebral cortex. Unexpectedly, these data suggest that neurogenesis was not enhanced by fluvastatin.

Thus, we further examined whether angiogenesis was affected by fluvastatin. In the peri-infarct cortex and basal ganglia, BrdU-positive cells that were positive for CD31 as a marker of endothelial cells could be detected (Figure 2c,2d). The number of BrdU/CD31-double-positive cells was significantly increased in fluvastatin-treated rats (Figure 2j). The percentage of BrdU/CD31-double-positive cells in total BrdU-positive cells was also increased in fluvastatin-treated rats (Figure 2k). Consistently, microangiography using FITC-conjugated albumin[11] also showed that microvessels were significantly increased in fluvastatin-treated rats only in the peri-infarct cortex and basal ganglia, without destruction of the blood–brain (Figure 3a to 3h). Quantitative analysis showed that the length and area of microvessels were also increased in the peri-infarct region, but not in the contralateral cortex and contralateral basal ganglia, in rats treated with fluvastatin, at 3 months after stroke (Figure 3i,j).

Because recent reports showed that neurite outgrowth was observed in the peri-infarct region from 7 to 14 days after cerebral infarction,[16,17] we next examined the effect of fluvastatin on neurite outgrowth. Immunohistochemical staining showed that treatment with fluvastatin significantly increased the immunoreactivity of MAP1B, a marker of neurite outgrowth, in neurites[16,18] (Figure 4), although the number of MAP1B-positive cells was the same in both groups. These data implied that the fluvastatin might promote angiogenesis, resulting in improvement of the microcirculation, and neurite outgrowth.

One possible explanation for the enhanced angiogenesis and neurite outgrowth is a decrease in oxidative stress by fluvastatin. To assess oxidative stress, we evaluated superoxide production using dihydroethidium staining (Figure 5a to 5e). Superoxide anion was increased in the ischemic core as compared with the contralateral region at 2 weeks after MCA occlusion (Figure 5a,5c). However, rats treated with fluvastatin showed a significant reduction in superoxide anion especially in the ischemic core region, but not in the peri-infarct cortex and basal ganglia (Figure 5b,5d,5e).

Finally, we examined Aβ deposition in the thalamic nuclei, because previous reports showed that Aβ deposits in the

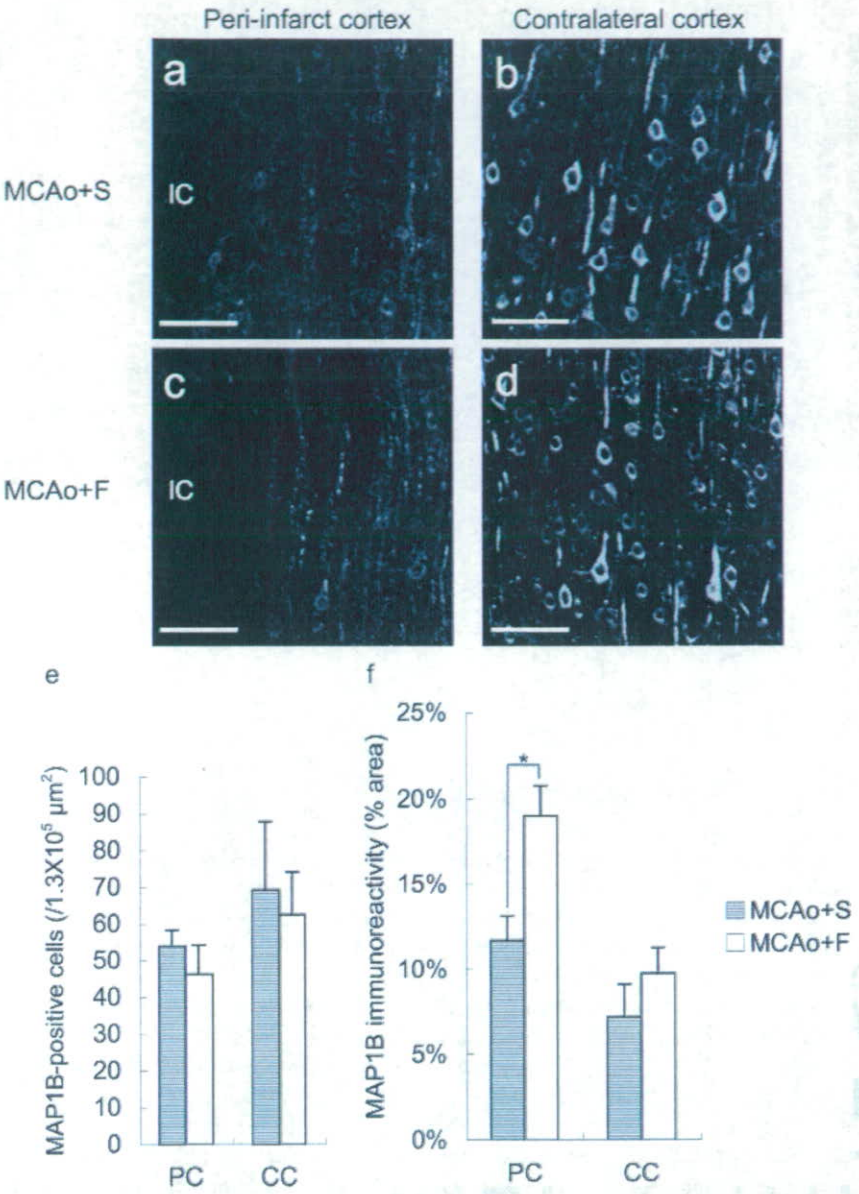

Figure 4. Typical images of immunohistochemical staining for MAP1B in peri-infarct cortex (a and c) and contralateral cortex (b and d) on day 14 (bar=100 μm). Although the number of MAP1B-positive cells was the same in both groups (e), immunoreactivity was higher in the peri-infarct region in fluvastatin-treated rats (f) (n=4 in each group, $^*P<0.05$).

thalamic nuclei persisted as long as 9 months after focal cerebral ischemia.[12] Although immunohistochemical staining showed marked deposition of Aβ in the ventrolateral and ventromedial thalamic nuclei at 3 months after stroke, the area of Aβ deposits was significantly decreased in fluvastatin-treated rats (Figure 5f to 5h). In other regions, such as cortex or basal ganglia, there was no Aβ deposits in both groups as reported before.[12]

Discussion

Although several laboratories have shown that long-term pretreatment with a statin reduces infarct size in rodents,[19] no articles have reported the effects of delayed postischemic treatment with statins. The present study demonstrated that statin treatment beginning 7 days after ischemic stroke resulted in significant improvement of spatial learning at 8 weeks after stroke, without any change in the plasma cholesterol level and infarct size.

Fluvastatin-treated rats showed a significant increase of MAP1B in neurites in the peri-infarct region. Considering that MAP1B is especially prominent in extending neurites[20] and related to functional recovery after ischemic stroke,[17] one of the possible effects of fluvastatin is to enhance neurite outgrowth, "neuritogenesis," in the early stage of treatment. This speculation might be supported by the recent study demonstrating that neurite outgrowth is accelerated by pravastatin via inhibiting the activity of geranylgeranylated proteins such as RhoA.[21]

As BrdU/CD31-positive cells were increased 14 days after MCAo and microvessels were also increased in the peri-infarct region 100 days after MCAo, fluvastatin enhanced angiogenesis and resulted in improvement of microcirculation in the peri-infarct region. Although the relationship between the improved microcirculation and behavior is still unclear, a recent report demonstrated that the restoration of perfusion by collateral growth and new capillaries in the

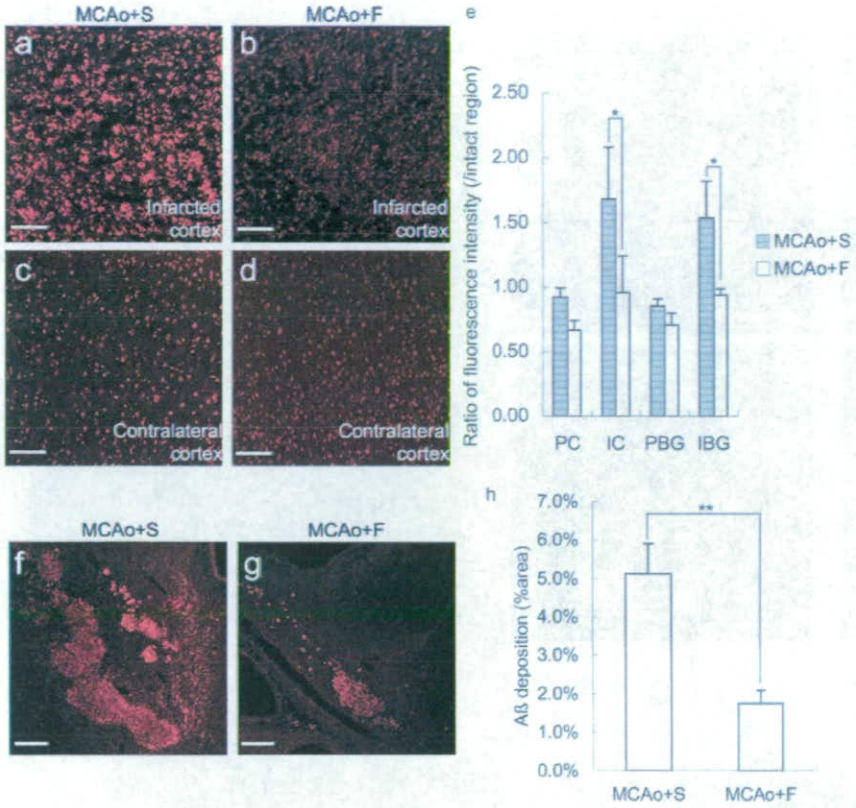

Figure 5. a through e, Superoxide anion detected by dihydroethidium staining on day 14. Red spots show the existence of superoxide anion. Fluorescence intensity was higher in the infarcted cortex (a) compared with the contralateral cortex (c). Fluvastatin-treated rats showed decreased fluorescence intensity in the infarcted cortex (b), although there was no difference in the peri-infarct cortex and basal ganglia (e) (n=4 in each group, $*P<0.05$, bar=100 μm). Deposition of Aβ in thalamus on day 100 after middle cerebral artery occlusion. Although deposition of Aβ was observed in the thalamic nuclei (f and g), there was no deposition in other regions such as the cortex and basal ganglia. Quantitative analysis showed decreased Aβ deposition in fluvastatin-treated rats (h) (n=6 in each group, $**P<0.01$, bar=200 μm).

ischemic border zone around a cortical infarct supported long-term functional recovery in rats.[22] Additionally, others reported that some patients who received tissue plasminogen activator therapy with no immediate clinical improvement despite early recanalization showed delayed clinical improvement.[23] From these viewpoints, it is likely that the improvement of microcirculation is an important factor for the functional recovery.

Of importance, fluvastatin reduced deposition of Aβ in the ventrolateral–ventromedial thalamic nuclei in the chronic stage of ischemic stroke, although rats subjected to focal cerebral ischemia develop deposition of Aβ in the ventroposterior lateral and ventroposterior medial nuclei for as long as 9 months.[12] This might be similar with precious reports showing that statins reduced the production of Aβ in Alzheimer disease.[24] The mechanism of the reduction of Aβ by fluvastatin should be further investigated.

Thus, the rats treated with fluvastatin showed enhancement of angiogenesis and neurite outgrowth in the peri-infarct cortex and reduced deposition of Aβ in the ventrolateral–ventromedial thalamic nuclei. Because those regions are important sites for spatial learning,[25,26] we speculate that the enhancement of functional recovery by fluvastatin might be dependent on those regions.

The other histological difference was the reduction of superoxide anion in the ischemic core in fluvastatin-treated rats. Because cerebral blood flow in the ischemic cortex remained to be reduced for 48 hours and restored to some extent 9 days after permanent MCAo,[27] we speculate that fluvastatin could reach the ischemic core and show the antioxidative effects. On the contrary, in the peri-infarct region, superoxide anion was not detected even in the control group and no effect of fluvastatin might be observed. This effect of statin is similar with the previous report showing that cerivastatin prevented the production of superoxide anion in the cerebral parenchyma in stroke-prone spontaneously hypertensive rats.[28] Also, fluvastatin is reported to possess antioxidative properties in other cells.[29,30]

The association of neurogenesis is also the center of interest, because previous reports showed an increase in neurogenesis after atorvastatin treatment beginning at 1 day after stroke.[5] However, we speculate that neurogenesis might not have contributed to the favorable outcome in the present study, because the volume of infarction was not decreased by fluvastatin, and the density of mature neurons (NeuN-positive cells) and proliferative immature neurons (BrdU/DCX-positive cells) was the same in both groups. From the viewpoints, the timing of treatment seems important for the enhancement of neurogenesis and the beginning of statin 7 days after MCAo might be too late to enhance neurogenesis.

The limitation of the present study is that there is no data demonstrating that fluvastatin crossed over the blood–brain barrier and acted on neurons directly. Blood–brain barrier permeability differs among statins and correlates in part with their respective lipophilicity.[31] Considering that pretreatment with pravastatin and rosuvastatin, whose lipophilicity is 0.84 and 0.33, respectively, shows significant effects on reducing infarction volume,[31] fluvastatin, whose lipophilicity is 1.27, might penetrate blood–brain barrier and have some direct effects on neurons. Otherwise, fluvastatin could penetrate the brain because of the disruption of blood–brain barrier after MCAo. One of other limitations in the present study is no

examination of the characteristics of BrdU positive-cells other than CD31, DCX, or NeuN. In addition, how these histological changes in fluvastatin-treated rats were mechanistically linked to improved outcome was not clarified. Further study is necessary to clarify these points.

Summary

Overall, delayed postischemic chronic fluvastatin treatment showed beneficial effects on the recovery of cognitive impairment after stroke by enhancement of neuritogenesis and of angiogenesis and a decrease in Aβ deposition and superoxide anion production. Further studies might show potential clinical utility to treat cognitive impairment in patients with ischemic stroke.

Acknowledgments

The authors thank Dr Masatsugu Horiuchi and Dr Masaru Iwai for their helpful advice on superoxide detection by dihydroethidium staining, and Dr Hiroshi Sato for assistance with MRI.

Sources of Funding

This work was partially supported by a Grant-in-Aid from the Organization for Pharmaceutical Safety and Research, a Grant-in-Aid from The Ministry of Public Health and Welfare, a Grant-in-Aid from Japan Promotion of Science, and a Grant-in-Aid from the Ministry of Education, Culture, Sports, Science, and Technology, of the Japanese Government.

Disclosures

Fluvastatin was donated from Novartis Pharma. Masataka Sata received Honoraria payment (modest) from Novartis Pharma. Ryuichi Morishita received honoraria payment (modest) and has an advisory board relationship to Novartis Pharma.

References

1. Sacks FM, Pfeffer MA, Moye LA, Rouleau JL, Rutherford JD, Cole TG, Brown L, Warnica JW, Arnold JM, Wun CC, Davis BR, Braunwald E. The effect of pravastatin on coronary events after myocardial infarction in patients with average cholesterol levels: cholesterol and recurrent events trial investigators. *N Engl J Med*. 1996;335:1001–1009.
2. Amarenco P, Tonkin AM. Statins for stroke prevention: disappointment and hope. *Circulation*. 2004;109:III44–49.
3. Moonis M, Kane K, Schwiderski U, Sandage BW, Fisher M. HMG-CoA reductase inhibitors improve acute ischemic stroke outcome. *Stroke*. 2005;36:1298–1300.
4. Chen J, Zhang C, Jiang H, Li Y, Zhang L, Robin A, Katakowski M, Lu M, Chopp M. Atorvastatin induction of VEGF and BDNF promotes brain plasticity after stroke in mice. *J Cereb Blood Flow Metab*. 2005;25:281–290.
5. Chen J, Zhang ZG, Li Y, Wang Y, Wang L, Jiang H, Zhang C, Lu M, Katakowski M, Feldkamp CS, Chopp M. Statins induce angiogenesis, neurogenesis, and synaptogenesis after stroke. *Ann Neurol*. 2003;53:743–751.
6. Zhang L, Zhang ZG, Ding GL, Jiang Q, Liu X, Meng H, Hozeska A, Zhang C, Li L, Morris D, Zhang RL, Lu M, Chopp M. Multitargeted effects of statin-enhanced thrombolytic therapy for stroke with recombinant human tissue-type plasminogen activator in the rat. *Circulation*. 2005;112:3486–3494.
7. Belayev L, Alonso OF, Busto R, Zhao W, Ginsberg MD. Middle cerebral artery occlusion in the rat by intraluminal suture: neurological and pathological evaluation of an improved model. *Stroke*. 1996;27:1616–1623.
8. Sata M, Nishimatsu H, Osuga J, Tanaka K, Ishizaka N, Ishibashi S, Hirata Y, Nagai R. Statins augment collateral growth in response to ischemia but they do not promote cancer and atherosclerosis. *Hypertension*. 2004;43:1214–1220.
9. Nakatomi H, Kuriu T, Okabe S, Yamamoto S, Hatano O, Kawahara N, Tamura A, Kirino T, Nakafuku M. Regeneration of hippocampal pyramidal neurons after ischemic brain injury by recruitment of endogenous neural progenitors. *Cell*. 2002;110:429–441.
10. Petullo D, Masonic K, Lincoln C, Wibberley L, Teliska M, Yao DL. Model development and behavioral assessment of focal cerebral ischemia in rats. *Life Sci*. 1999;64:1099–1108.
11. Cavaglia M, Dombrowski SM, Drazba J, Vasanji A, Bokesch PM, Janigro D. Regional variation in brain capillary density and vascular response to ischemia. *Brain Res*. 2001;910:81–93.
12. van Groen T, Puurunen K, Maki HM, Sivenius J, Jolkkonen J. Transformation of diffuse beta-amyloid precursor protein and beta-amyloid deposits to plaques in the thalamus after transient occlusion of the middle cerebral artery in rats. *Stroke*. 2005;36:1551–1556.
13. Iwai M, Liu HW, Chen R, Ide A, Okamoto S, Hata R, Sakanaka M, Shiuchi T, Horiuchi M. Possible inhibition of focal cerebral ischemia by angiotensin II type 2 receptor stimulation. *Circulation*. 2004;110:843–848.
14. Robinson RG. Differential behavioral and biochemical effects of right and left hemispheric cerebral infarction in the rat. *Science*. 1979;205:707–710.
15. DeVries AC, Nelson RJ, Traystman RJ, Hurn PD. Cognitive and behavioral assessment in experimental stroke research: Will it prove useful? *Neurosci Biobehav Rev*. 2001;25:325–342.
16. Badan I, Platt D, Kessler C, Popa-Wagner A. Temporal dynamics of degenerative and regenerative events associated with cerebral ischemia in aged rats. *Gerontology*. 2003;49:356–365.
17. Badan I, Dinca I, Buchhold B, Suofu Y, Walker L, Gratz M, Platt D, Kessler CH, Popa-Wagner A. Accelerated accumulation of n- and c-terminal beta app fragments and delayed recovery of microtubule-associated protein 1b expression following stroke in aged rats. *Eur J Neurosci*. 2004;19:2270–2280.
18. Schabitz WR, Berger C, Kollmar R, Seitz M, Tanay E, Kiessling M, Schwab S, Sommer C. Effect of brain-derived neurotrophic factor treatment and forced arm use on functional motor recovery after small cortical ischemia. *Stroke*. 2004;35:992–997.
19. Endres M, Laufs U, Liao JK, Moskowitz MA. Targeting enos for stroke protection. *Trends Neurosci*. 2004;27:283–289.
20. Gonzalez-Billault C, Avila J, Caceres A. Evidence for the role of map1b in axon formation. *Mol Biol Cell*. 2001;12:2087–2098.
21. Pooler AM, Xi SC, Wurtman RJ. The 3-hydroxy-3-methylglutaryl co-enzyme a reductase inhibitor pravastatin enhances neurite outgrowth in hippocampal neurons. *J Neurochem*. 2006;97:716–723.
22. Wei L, Erinjeri JP, Rovainen CM, Woolsey TA. Collateral growth and angiogenesis around cortical stroke. *Stroke*. 2001;32:2179–2184.
23. Alexandrov AV, Hall CE, Labiche LA, Wojner AW, Grotta JC. Ischemic stunning of the brain: Early recanalization without immediate clinical improvement in acute ischemic stroke. *Stroke*. 2004;35:449–452.
24. Fassbender K, Simons M, Bergmann C, Stroick M, Lutjohann D, Keller P, Runz H, Kuhl S, Bertsch T, von Bergmann K, Hennerici M, Beyreuther K, Hartmann T. Simvastatin strongly reduces levels of Alzheimer's disease beta -amyloid peptides Abeta 42 and Abeta 40 in vitro and in vivo. *Proc Natl Acad Sci U S A*. 2001;98:5856–5861.
25. Casu MA, Wong TP, De Koninck Y, Ribeiro-da-Silva A, Cuello AC. Aging causes a preferential loss of cholinergic innervation of characterized neocortical pyramidal neurons. *Cereb Cortex*. 2002;12:329–337.
26. Jeljeli M, Strazielle C, Caston J, Lalonde R. Effects of ventrolateral-ventromedial thalamic lesions on motor coordination and spatial orientation in rats. *Neurosci Res*. 2003;47:309–316.
27. Rudin M, Baumann D, Ekatodramis D, Stirnimann R, McAllister KH, Sauter A. MRI analysis of the changes in apparent water diffusion coefficient, t(2) relaxation time, and cerebral blood flow and volume in the temporal evolution of cerebral infarction following permanent middle cerebral artery occlusion in rats. *Exp Neurol*. 2001;169:56–63.
28. Kawashima S, Yamashita T, Miwa Y, Ozaki M, Namiki M, Hirase T, Inoue N, Hirata K, Yokoyama M. HMG-CoA reductase inhibitor has protective effects against stroke events in stroke-prone spontaneously hypertensive rats. *Stroke*. 2003;34:157–163.
29. Sumi D, Hayashi T, Thakur NK, Jayachandran M, Asai Y, Kano H, Matsui H, Iguchi A. A HMG-CoA reductase inhibitor possesses a potent anti-atherosclerotic effect other than serum lipid lowering effects–the relevance of endothelial nitric oxide synthase and superoxide anion scavenging action. *Atherosclerosis*. 2001;155:347–357.
30. Morita H, Saito Y, Ohashi N, Yoshikawa M, Katoh M, Ashida T, Kurihara H, Nakamura T, Kurabayashi M, Nagai R. Fluvastatin ameliorates the hyperhomocysteinemia-induced endothelial dysfunction: The antioxidative properties of fluvastatin. *Circ J*. 2005;69:475–480.
31. Endres M. Statins and stroke. *J Cereb Blood Flow Metab*. 2005;25:1093–1110.

Table I. Statistics in Morris Water Maze

	Hidden Test			Visible Test		
	Latency	Length	Speed	Latency	Length	Speed
P values in 2-factor repeated-measure ANOVA (Sham, MCAo+S, MCAo+F)						
Treatment	<0.001	<0.001	0.053	0.004	0.021	0.342
Day	<0.001	0.011	<0.001	0.003	0.014	0.288
Treatment×Day	0.002	<0.001	0.855	0.465	0.684	0.306
P values in Scheffe test on day 4						
Sham vs MCAo+S	<0.001	<0.001	0.933	0.018	0.025	0.585
Sham vs MCAo+F	0.024	0.010	0.277	0.138	0.058	0.266
MCAo+S vs MCAo+F	0.012	0.023	0.129	0.643	0.941	0.820

MCAo+S indicates saline-treated rats after MCAo; MCAo+F, fluvastatin-treated rats after MCAo.

CARDIAC PRACTICE

別　刷

(株)メディカルレビュー社

目でみるページ・検査

diffusion MRI

国立循環器病センター研究所先進医工学センター先進診断機器開発室室長　佐藤　博司 Sato, Hiroshi
同　循環動態機能部室長　稲垣　正司 Inagaki, Masashi
同　放射線医学部室長　林　拓也 Hayashi, Takuya
同　部長　飯田　秀博 Iida, Hidehiro

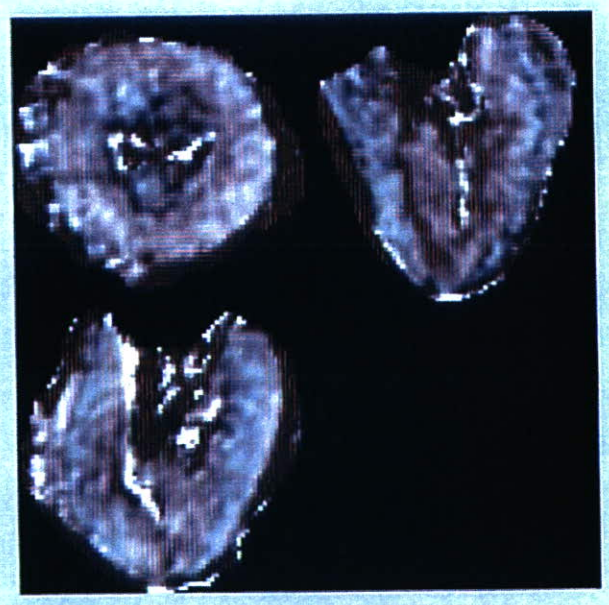

図1　diffusionテンソル解析によるprincipal diffusion direction
HB犬(34ヵ月齢，体重25kg，死後)胸部に対して，GE社製MRI装置SIGNA EXCITE HD(3T)，カーディアック用8チャンネルフェーズドアレイコイルを用いてdiffusion MRIを行った。撮像パラメータはSE-EPI法，4 Shot，TR10,500(ms)，TE68.2(ms)，空間解像度1.5mm，バンド幅1.3kHz/pix，加算12回，b値1,000(s/mm^2)を用い，スキャン時間は5時間30分であった。diffusionの情報は方向性をもつため，空間の各方向に対して等方的に31方向のdiffusionスキャンを行い，それぞれの位置に対するテンソルを求めた。最大の固有値をもつ固有ベクトルの方向＝PDD（principal diffusion direction）は，線維方向を反映していると考えられる。赤い線の方向はPDDを示し，空間的異方性の強さを画素の輝度で表現した画像にオーバーレイされている。左上は短軸断面像を示し，その右と下はその直交した断面を示している。短軸断面像においてPDDが接線方向を示しており，これまでの筋肉の線維方向の知見と一致した。筋肉は神経線維に比べて異方性が低く，また脳に比べて動きなどの影響や，他の臓器からのアーチファクトの混入が大きいため，臨床応用が困難である。心臓領域におけるdiffusion MRIが実用化されるためには，MRIの傾斜磁場の性能の向上や撮像シーケンスの最適化が必須である。

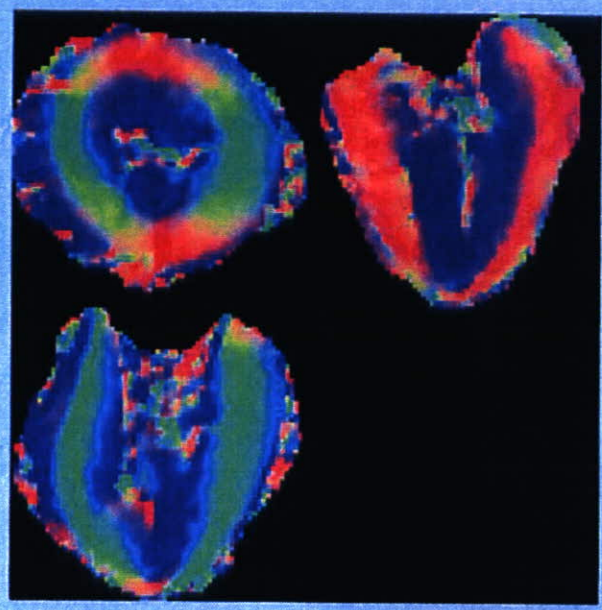

図2　Three dimensional anisotropy contrast MRI
図1におけるテンソル固有値解析において，最大の固有値をもつ固有ベクトルの直交する方向成分をRGBの輝度情報として表示したものである。青色はPDDが長軸方向であることを示し，緑色と赤色は短軸面でそれぞれが直交する方向を示している。これらの3軸以外の斜めの方向は，それぞれの色が混ざることにより表現されている。線による方向表示(図1)よりもPDDの方向分布を直感的に把握しやすい。

図3　MYLT(MYocardial fiber Layered Tractography)法による線維連絡の可視化
diffusion MRIのもつ情報は，これまでのT_1強調像，T_2強調像のように単純に輝度情報に置き換えられるものではなく，よりたくさんの情報をもつため，臨床上有意な情報をいかに可視化していくかが重要な問題となる。当センターではそのための手段としてMYLT法を開発した。心筋内膜側のある関心領域を出発点として，異方性をもつ情報から統計的に有意な線維連絡の確率分布を求め，それぞれの方向からその確率の最大値投影を行う(赤色)。同様に心筋外膜側を出発点としたものを青色，中間からのものを緑色で示し，b値0 (s/mm^2)の断層像にオーバーレイしている。心筋中央部の線維が短軸に対し円状となり，外膜，内膜側はそれぞれ逆の角度をもったらせん状の走行を示していることがわかる。

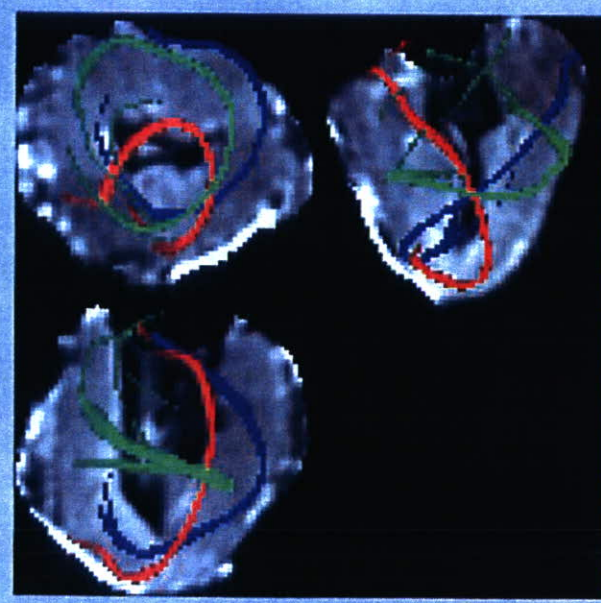

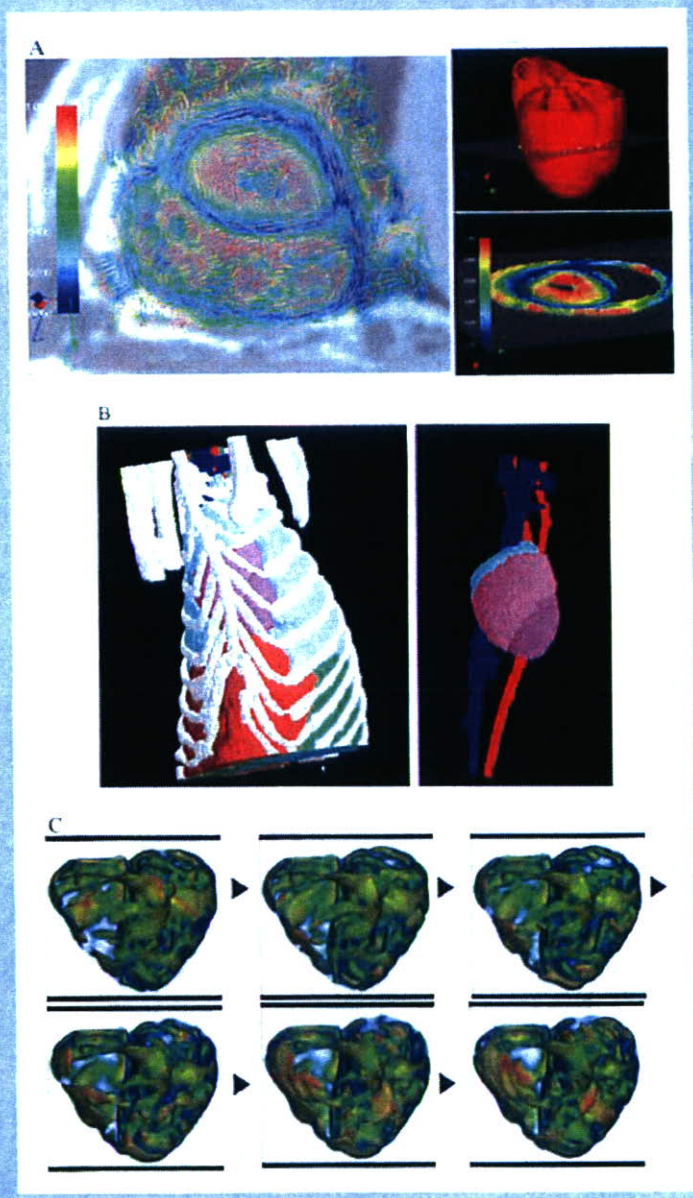

図4　DTMRIにより計測された心筋線維方向を用いた心臓のコピュータ・シミュレーション

心臓における電気的興奮伝播や心室収縮には心筋線維方向が大きく影響する。筆者らはMRIを用いて計測した心臓形状・心筋線維方向をもとに，イオンチャンネルや収縮蛋白の数理モデルから心電図・心室収縮までのマルチフィジックス・マルチスケール心臓シミュレーションを行っている(東京大学・久田研究室との共同研究)。

A：DTMRIにより計測されたイヌ心臓の心筋線維方向(青：心室短軸円周方向～赤：長軸方向)。

B：MRI画像をもとに作製したイヌの胸郭モデル(左)および心臓・大血管モデル(右)。

C：心筋線維方向を導入した心臓モデルによる心室細動中の電気的興奮波のシミュレーション。多数の渦巻き様興奮波が生じている。

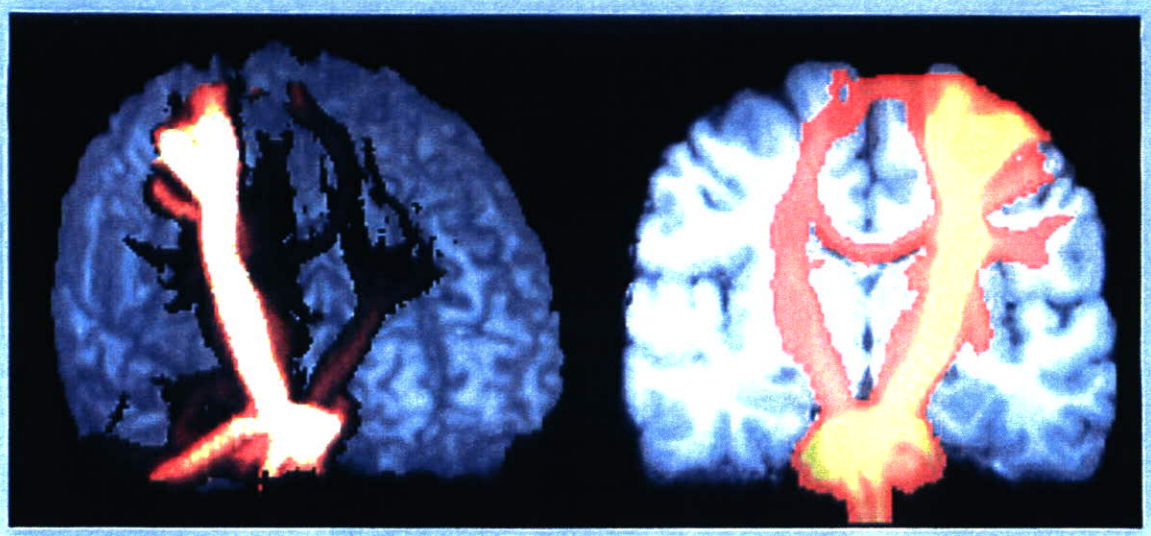

図5　脳におけるトラクトグラフィ
MRI拡散強調画像により，脳内水分子の方向依存性の拡散移動度を測定することで脳内の各画素における神経線維方向が推定でき，隣同士の画素の線維方向をつなげることで線維追跡を行うことができるようになった。近年，撮像技術や解析法の進歩によって高空間・高方向解像度の画像収集や拡散方向推定モデルの改善が進み，線維追跡感度が向上している。上図は大脳皮質運動野の線維連絡追跡結果を示す。

Heart and Brain Circulation and CO2 in Healthy Men

Ikuo Yokoyama M.D.[a,e], Yusuke Inoue M.D.[b] ,Toshibumi Kinoshita M.D.[c], Hiroshi Itoh M.D.[c,d], Iwao Kanno,[c,d], Hidehiro Iida PhD., Dsc [d, e]

[a] Department of Cardiovascular Medicine, Sanno Hospital, International University of Health and Welfare, Tokyo, Japan, [b] Department of Radiology, Institute of Medical Science, Graduate School of Medicine University of Tokyo, Tokyo, Japan, [c] Department of Radiology Akita Research Institute of Brain and Blood Vessels, Akita, Japan, [d] Brain Imaging Project, National Institute of Radiological Sciences, [e] Department of Radiology, the Research Institute of National Cardiovascular Center, Osaka, Japan.

Address for correspondence;

Ikuo Yokoyama M.D.

Correspondence to: Dr Ikuo Yokoyama, Department of Cardiovascular Medicine, Sanno Hospital, International University of Health and Welfare, 8-10-16 Akasaka, Minato-ku, Tokyo 107-0052, Japan

TEL: +81-3-3402-3151

FAX: +81-3-3404-3652

E-mail: yokochan-tky@umin.ac.jp

Received: 21/10/07

Revision Requested: 3/12/2007

Revision Received: 1/2/2008

Accepted: 8/2/2008

Short title: Heart and Brain Perfusion and CO2

doi: 10.1111/j.1748-1716.2008.01846.x

Abstract

Aim: To compare blood flow response to arterial carbon dioxide tension change in the heart and brain of normal elderly men.

Methods: Thirteen healthy elderly male volunteers were studied. Hypercapnea was induced by carbon dioxide inhalation and hypocapnea was induced by hyperventilation. Myocardial blood flow ($mL*minute^{-1}*[100\ gram\ of\ perfusable\ tissue]^{-1}$) and cerebral blood flow ($mL*minute^{-1}*[100\ gram\ of\ perfusable\ tissue]^{-1}$) were measured simultaneously at rest, under carbon-dioxide gas inhalation and hyperventilation using the combination of two positron emission tomography scanners.

Results: Arterial carbon dioxide tension increased significantly during carbon dioxide inhalation (43.1±2.7 mmHg, $p < 0.05$) and decreased significantly during hyperventilation (29.2±3.4 mmHg, $p< 0.01$) from baseline (40.2±2.4 mmHg). Myocardial blood flow increased significantly during hypercapnea (88.7±22.4, $p < 0.01$) from baseline (78.2±12.6), as did the cerebral blood flow (baseline: 39.8±5.3 vs. hypercapnea: 48.4±10.4, $p < 0.05$). During hypocapnea cerebral blood flow decreased significantly (27.0±6.3, $p < 0.01$) from baseline as did the myocardial blood flow (55.1±14.6, $p < 0.01$). However normalized myocardial blood flow by cardiac workload ($100mL*mmHg^{-1}*[heart\text{-}beat]^{-1}*[gram\ of\ perfusable\ tissue]^{-1}$) was not changed from baseline (93.4±16.6) during hypercapnea (90.5±14.3) but decreased significantly from baseline during hypocapnea (64.5±18.3, $p < 0.01$).

Conclusion: In normal elderly men, hypocapnea produces similar vasoconstriction in both heart and brain. Mild hpercapnea increased cerebral blood flow but did not have an additional effect to dilate coronary arteries beyond the expected range in response to an increase in cardiac workload.

Key Words: Carbon dioxide, Coronary circulation, Cerebrovascular circulation, Hypercapnea, Hyperventilation, Hypocapnea, Myocardial blood flow, Positron emission tomography

Introduction

Correlation between arterial carbon dioxide tension and cerebral blood flow is well established [Kety & Schmidt 1948, Shimosegawa et al. 1995, Kuwabara et al. 1997]. However, responsiveness of myocardial blood flow to hypercapnea and hypocapnea has not been fully elucidated. These relationships were investigated in animal experiments [Feinberg et al. 1960, Love et al. 1965, Case & Greenberg 1976, Bos et al. 1979, Powers et al. 1986] and human clinical studies [Rowe et al. 1962, Neill & Hattenhauer 1975, Wilson et al. 1981, Kazmaier et al. 1998] with conflicting results. The inconsistencies observed should be attributable to differences in experimental conditions, such as the techniques used for measurement, or whether the studies were performed in animals or humans, or presence versus absence of ischemic heart disease.

In this study, we evaluated the responses of myocardial blood flow and cerebral blood flow to hypercapnea and hypocapnea in healthy elderly men. We employed a dual positron emission tomography (PET) scanner consisting of two scanners to measure myocardial blood flow and cerebral blood flow simultaneously in the same subject [Iida et al. 1998]. PET allows assessment of functional parameters under physiological conditions. Using this dual PET scan technique allowed simultaneous assessment of myocardial and cerebral circulations, noninvasively and reliably and enabled comparison of the two.

Materials and Methods

Study Subjects

Thirteen healthy men (age range 51-71 years; mean 59.4, standard deviation [5.5]) who had been the subjects of previously published studies with different objectives [Iida et al. 1998, Ito et al. 1999, Ito et al. 2000, Ito et al. 2002] took part in the study. These men had normal laboratory parameters, no signs or symptoms of ischemia in the heart or brain, and no abnormalities were found by brain magnetic resonance imaging, electrocardiography, cardiac echocardiography, and physical examination. All subjects provided written informed consent that data obtained from the PET studies could be used for research purposes. The study protocol was approved by the Ethics Committee of the Research Institute of Brain and Blood Vessels, Akita, Japan.

PET Procedures

The Headtome V dual PET system (Shimadzu Corp., Kyoto, Japan), a combination of the two Headtome V PET scanners, was used for all studies [Iida et al. 1998]. The system allowed simultaneous imaging of the brain and heart and provided 47 sections for the brain and 31 sections for the heart with center-to-center distances of 3.125 mm. The intrinsic spatial resolution was 4.0 mm in-plane and 4.3 mm full-width at half-maximum axially. All PET data were acquired in 2D mode and reconstructed with a Butterworth filter, resulting in a final in-plane resolution of approximately 8 mm full-width at half-maximum.

After an overnight fast, subjects were placed in the supine position on the scanner bed. The blood-pool images were obtained 1 minute after continuous inhalation of ^{15}O-CO gas (approximately 5 GBq total applied to the mouth). One minute after the end of ^{15}O-CO gas inhalation, ^{15}O-CO blood-pool images of the heart were obtained with an R-wave triggered electrocardiogram gated tomographic scan. A simultaneous gated static scan on both the heart and brain was done 4 minutes after the inhalation of ^{15}O-CO gas. Three venous blood samples were taken during the ^{15}O-CO scan, and the radioactivity concentration in the whole blood was measured using a NaI-well counter that was cross-calibrated with the PET scanner. ^{15}O-CO blood-pool images were used to draw regions of interests on left ventricular cavity and left ventricular wall accurately to obtain time activity curves. The recovery of